Adsorption and Reaction in Single-File Networks

Peter Bräuer, Andreas Brzank, and Jörg Kärger*

Universität Leipzig, Fakultät für Physik und Geowissenschaften, Linnéstrasse 5, D-04103 Leipzig, Germany

Received: August 21, 2002; In Final Form: December 10, 2002

The possibility of reactivity enhancement by molecular traffic control (MTC) is rationalized by dynamic Monte Carlo simulations in a network of single-file systems. The obtained dependencies may be explained by the peculiarities of molecular propagation in single-file systems and interpreted in a semiquantitative way by adopting a suitable modification of the Thiele concept for evaluating the effectiveness of catalytic reaction under transport limitation. Though the benefit of the so far considered MTC systems has to be purchased by a number of shortcomings, including additional transport inhibition and reduced concentration of reactive sites, there appear to exist promising routes to more complex single-file networks affording reactivity enhancement by molecular traffic control under practically acceptable conditions.

I. Introduction

The mutual correlation in the movement of the constituents of multicomponent fluids is one of the intriguing features of fluid dynamics. Under the influence of confining walls, the complexity of the interactions between diffusing components of the fluid may be substantially enhanced. In pore channels with diameters slightly exceeding the molecular diameters, long-range correlation in the movement of the individual molecules are known to lead to molecular propagation patterns notably deviating from normal diffusion. Molecular transport under this type of confinement has been termed single-file diffusion.[1−4]

Mutually intersecting arrays of single-file systems can serve as a model system for the simulation of reactivity enhancement by confinement, the phenomenon of so-called "molecular traffic control" (MTC).[5,6] The expression MTC has been chosen to describe chemical reactions in nanoporous materials where reactant and product molecules prefer different pathways for their diffusion. Important examples of materials, which might exhibit such a behavior, are zeolites of MFI structure type like ZSM-5.[7] Such zeolites contain two different types of mutually intersecting channels. Molecular dynamic simulations of gas adsorption of two components in silicalite-1,[8] in boggsite zeolite (BOG),[9] and in faujasite (FAU)[10] have in fact shown that the residence probability in different areas of the intracrystalline pore space may be notably different for the two fluid components. The concept of MTC implies that the difference in the residence probabilities of reactant and product molecules in the two channel systems causes a reduced transport inhibition, which in the case of transport-controlled reactions[11,12] leads to an enhanced output of product molecules. The MTC effect has remained a subject of controversial discussions over two decades in the literature[6,12−16] and did not find up to now a theoretical foundation.

II. Simulation Model

We consider a quadratic lattice (cf. Figure 1) consisting of $n_\alpha = n_\beta = n$ channels of type α (○) and β (□). The number of sites between two neighboring channel intersections (×) and between a channel intersection and a marginal lattice point (△), respectively, is l. The total number of sites in a channel is

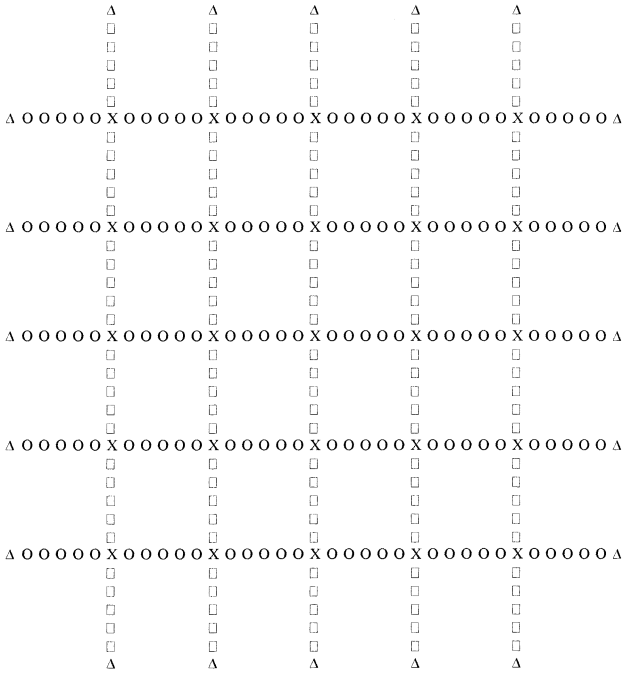

Figure 1. Quadratic lattice consisting, as an example, of $n_\alpha = 5$ channels of type α (○) and of $n_\beta = 5$ channels of type β (□) with $l = 5$ sites between the intersections. The intersections of the channels are characterized by the symbol × and the marginal lattice sites by △, respectively.

$$m = (n + 1)l + n + 2 \tag{1}$$

the number of intersections

$$m_c = n^2 \tag{2}$$

and the total number of all sites

$$m_{tot} = 2nm - m_c = n[2(n + 1)l + n + 4] \tag{3}$$

For the lattice in Figure 1, it holds that $n_\alpha = n_\beta = n = 5$; $l =$

* To whom correspondence should be addressed.

10.1021/jp021911t CCC: $25.00
Published on Web 02/04/2003

5; $m = 37$; $m_c = 25$; and $m_{tot} = 345$. Each site of the lattice can be occupied by only one particle.

Within the network, the channel intersections give rise to a unidirectional molecular reaction A → B with the rate of reaction

$$dN_A/dt = -k_c N_A \tag{4}$$

where N_A is the number of the reactant molecules of type A and $k_c = \kappa_c/\tau$ is the site reaction rate. τ denotes the length of an elementary time step of simulation. Therefore, the meantime necessary for conversion of the reactant molecule A to the product molecule B is equal to τ/κ_c. κ_c represents the reaction probability at an intersection point. By means of the following relationship, one can introduce the average reactivity of the lattice (i.e., the reactivity per lattice point):

$$\langle k \rangle = k_c \frac{m_c}{m_{tot}} = \frac{\kappa_c}{\tau}\frac{m_c}{m_{tot}} = \frac{\kappa_c}{\tau}\frac{m_c}{2nm - m_c} = \frac{\kappa_c}{\tau}\frac{n}{2(n+1)l + n + 4} \tag{5}$$

The time unit τ of the simulation is set equal to the mean value of the time interval between subsequent jump attempts of one and the same particle. These time intervals are identical for the A and B molecules and can be formally set equal to one.

We consider two kinds of lattices. In the case of the so-called molecular traffic control system (MTC system), molecular entrance to the channels from the marginal lattice points and the intersections is subjected to the respective probabilities $P_{A,\alpha}$, $P_{A,\beta}$, $P_{B,\alpha}$, and $P_{B,\beta}$, which possess values between zero and one and which have to be considered, depending on the direction of the statistically selected jump attempt. In the case of the so-called "hard" MTC system, which is predominantly regarded in the present communication, one has $P_{A,\alpha} = 1$, $P_{A,\beta} = 0$, $P_{B,\alpha} = 0$, $P_{B,\beta} = 1$, i.e., the molecules of type A can only occupy the α channels, and the molecules of type B can only occupy the β channels. In the case of the so-called reference system (REF system), both channel types are equally accessible by both types of molecules. The simulations were started with a random distribution of the molecules of set A over the lattice, i.e., for the MTC system inside the α channels and for the REF system in both the α and β channels. The wanted average initial occupation $\langle \Theta_A(t = 0) \rangle$ of the lattice with reactant molecules of type A is achieved[17] by addressing all sorts of lattice points (in the "hard" MTC system only those in the α-channels) by a random number z with $0 \le z \le 1$. For $z < \langle \Theta_A(t = 0) \rangle$, the lattice point will be occupied, and conversely, for $z \ge \langle \Theta_A(t = 0) \rangle$, it will remain empty. Obviously, the initial occupations of the "hard" MTC system and of the REF system by molecules of type A are interrelated by

$$\langle \Theta_A^{MTC}(t = 0) \rangle / nm = \langle \Theta_A^{REF}(t = 0) \rangle / m_{tot} \tag{6}$$

For the sake of a better comparability, we have thus overcome the deficiency of preliminary simulations,[18−20] where the total molecular concentrations in the MTC and REF systems have artificially been kept identical.

The steady state is considered to be attained as soon as, with evolving simulation time, the average number of molecules of type B on the lattice remains constant. For studying the internal dynamics of the system, now all particles within the system are labeled. Their average numbers are denoted $N_{A,lab}(t)$ and $N_{B,lab}(t)$, respectively. Particles, entering the system later are considered to be unlabeled. Correspondingly, their average numbers are denoted $N_{A,unlab}(t)$ and $N_{B,unlab}(t)$, respectively. Additionally, we have counted also those molecules that are converted from labeled molecules of type A to those of type B. Their average number is named $N_{B,lab}^{new}(t)$. The respective average particle numbers are interrelated in the following way:

$$N_{A,tot}(t) = N_{A,lab}(t) + N_{A,unlab}(t); \qquad N_{B,tot}(t) = N_{B,lab,tot}(t) + N_{B,unlab}(t)$$

$$N_{B,lab,tot}(t) = N_{B,lab}(t) + N_{B,lab}^{new}(t); \qquad N_{AB,tot}(t) = N_{A,tot}(t) + N_{B,tot}(t) \tag{7}$$

We assume that the systems are surrounded by a gas stream, which contains only molecules of type A. Desorbing molecules of type B, which originate from molecules of type A, are spilled out by the surrounding gas stream. In the simulation, this is achieved by removing all B molecules from marginal sites after each simulation step. Further, we assume that the marginal lattice sites have lost the memory of their occupation after any jump to or from them;[17,21] that is, the adsorption or desorption of molecules of type A at the marginal lattice sites takes place without consideration of the present occupation of the margins after each jump attempt with the probabilities $\langle \Theta_A(t = 0) \rangle$ or $1 - \langle \Theta_A(t = 0) \rangle$ at any lattice site, respectively. Thus, in contrast to the molecules of type B, molecules of type A have the chance to remain on the marginal lattice sites and thus to jump into the lattice during the next simulation step. Jump attempts in any of the four directions were carried out with the probability $^1/_4$. Jump attempts from any channel site perpendicular to the channel direction, i.e., toward the matrix of the catalyst, and jumps to an occupied neighboring lattice site leave the system in its given state. At the intersections, the molecules of type A have the possibility to be converted into the product molecules of type B as well as to jump to empty neighboring lattice points. To keep the simulation scheme as simple as possible, the possibilities of molecular reaction and molecular jumps are considered in subsequent order. In doing so, we neglect the effect of jump time and reaction time distributions. The resulting deviations, however, are known[22,23] to be of minor influence, which will not effect the general trends of the simulations.

The simulations were finished when the average number of labeled particles of type B, $N_{B,lab}(t)$, dropped to zero. In cases, where the exchange time turned out to be too long, the simulations were stopped, when the concentration of the labeled molecules of type B dropped to 5%. These cases shall be specially indicated (see section V).

All simulations were repeated 1000 times with different sequences of random numbers; that is, all calculated values are averages over 1000 equal systems. The pseudorandom numbers used in the simulations were generated using a sophisticated algorithm introduced by Marsaglia.[25] More simple random number generators turned out to be insufficient in some cases and had therefore to be abandoned.[17,26]

As an example, Figure 2 shows typical curves for the development of average particle numbers over 1000 elementary time steps after reaching the steady state for a lattice with $n = 5$; $l = 5$ (cf. Figure 1) and a reaction probability $\kappa_c = 0.1$ for the MTC system (Figure 2a) and for the REF system (Figure 2b). The average initial occupation of the lattice with reactant molecules of type A in the REF system is $\langle \Theta_A(t = 0) \rangle = 0.25$. $N_{AB,tot} = 86.01 \pm 0.60$ is the calculated average total number of molecules in the REF system. This value is in complete agreement with $N_{AB,tot,exact} = m_{tot} \langle \Theta_A(t = 0) \rangle = 345 * 0.25 = 86.25$, which results from the analytical expression of m_{tot} (eq 3) and the fact that in the REF system the total concentration cannot be affected by internal reactions of the considered type.[19]

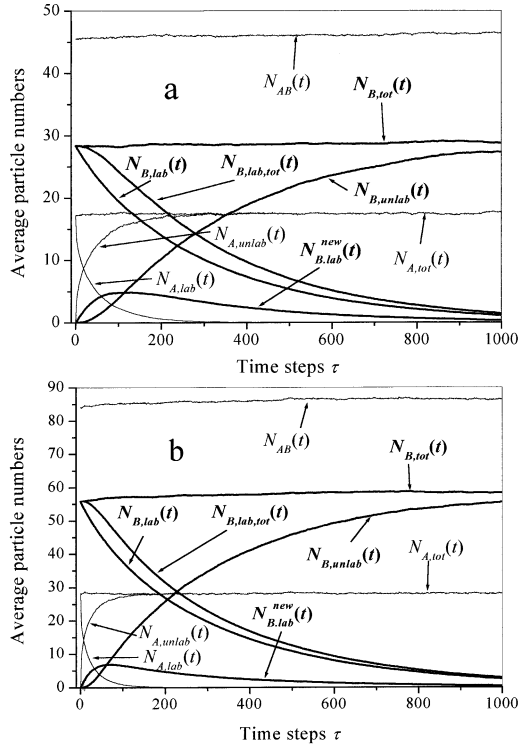

Figure 2. Time development of average particle numbers over 1000 elementary time steps after reaching the steady state for a lattice with $n = 5$; $l = 5$ (cf. Figure 1) and a reaction probability $\kappa_c = 0.1$ for the MTC system (a) and the REF system (b). As a help for the eyes, the various time dependences for particles B are represented by thicker lines.

Although the dependencies are generally found to decrease or increase monotonically, only the function $N^{new}_{B,lab}(t)$ passes a maximum (cf. Figure 2). This is a simple consequence of the fact that the "source" of $N^{new}_{B,lab}$, the labeled reactant molecules $N_{A,lab}$, disappears.

III. Reactivity Enhancement by Molecular Traffic Control

For a lattice with $n = 3$ α and β channels, we have calculated the outputs of B molecules per lattice site and per elementary time step for the MTC system (ξ_B^{MTC}) and for the REF system (ξ_B^{REF}) in dependence on the number l of sites between two neighboring intersection points for a reaction probability $\kappa_c = 0.5$ and for the initial lattice occupation $\langle\Theta_A(t = 0)\rangle = 0.25$. Figure 3a shows the ratio of these outputs ξ_B^{MTC}/ξ_B^{REF} as a function of l. Obviously, for small values of l, the output in the REF system is greater than in the MTC system, whereas for $l > 6$, the ratio is becoming larger than one, making the MTC system more favorable than the REF system. As an example, Figure 3b shows the ratio between the effective reactivities of the MTC and the REF system for $l = 1$ as a function of the total amount n of α and β channels. It passes a maximum for $n = 2$. Even in this point the ratio is notably less than one, indicating that in this case the efficiency of the MTC system is notably inferior to that of the REF system. This is to be expected on the basis of Figure 3a, where for small values of l (and in particular for $l = 1$) this ratio has been found to be distinctly smaller than 1. In Figure 3b it is exhibited that the further enhancement of n monotonically further impairs rather than improves the benefit of the MTC system in comparison with the reference system.

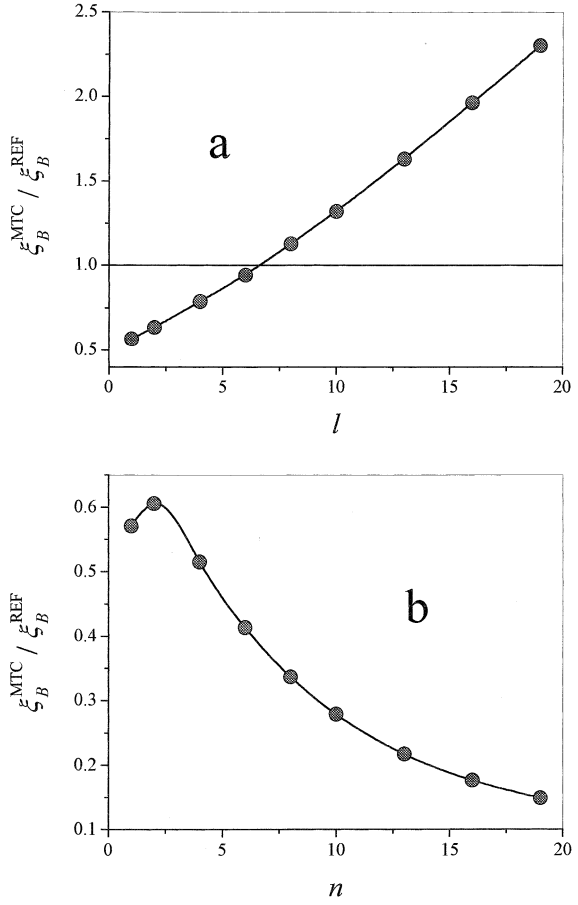

Figure 3. Benefit ξ_B^{MTC}/ξ_B^{REF} of the MTC system in comparison with the REF system for $n = 3$ as a function of the number l of sites in the channel segments between two neighboring intersections (a) and for $l = 1$ in dependence on the number n of α and β channels (b). In both graphs, the curves were calculated for a reaction probability $\kappa_c = 0.5$ and an initial lattice occupation $\langle\Theta_A(t = 0)\rangle = 0.25$.

It shall be the task of the subsequent sections to elucidate in more detail the conditions that are responsible for the efficiency of the MTC and REF systems relative to each other.

IV. Concentration Profiles and Average Occupation Numbers

Figures 4−6 show the distribution of the A molecules (a and d), of the B molecules (b and e), and of both molecules (c and f) in the α and β channels for the initial occupation of the lattice $\langle\Theta_A(t = 0)\rangle = 0.25$ in the case of the MTC system (Figures 4−6, parts a−c in each) and the REF system (Figures 4−6, parts d−f in each) for three different reaction probabilities $\kappa_c = 0.01$ (Figure 4), 0.1 (Figure 5), and 1 (Figure 6). The lattice consists of $n = 5$ α and β channels and $l = 5$ sites between the channel intersections (cf. Figure 1). As expected for transport-dependent processes, in both the MTC and REF systems, the concentration of the reactant molecules decreases toward the network center (Figures 4−6, parts a and d in each), whereas concentration of the product molecules decreases toward the margins of the lattice (Figures 4−6, parts b and e in each). As a remarkable feature, in contrast to the behavior of the REF system (Figures 4−6, parts f in each), where the total concentration of the molecules A and B is constant all over the lattice, molecular traffic control (Figures 4−6, parts c in each) leads to a pronounced deviation from a constant occupancy over the network. Comparing Figures 4−6, all of the considered effects are found to be much more pronounced for larger reaction

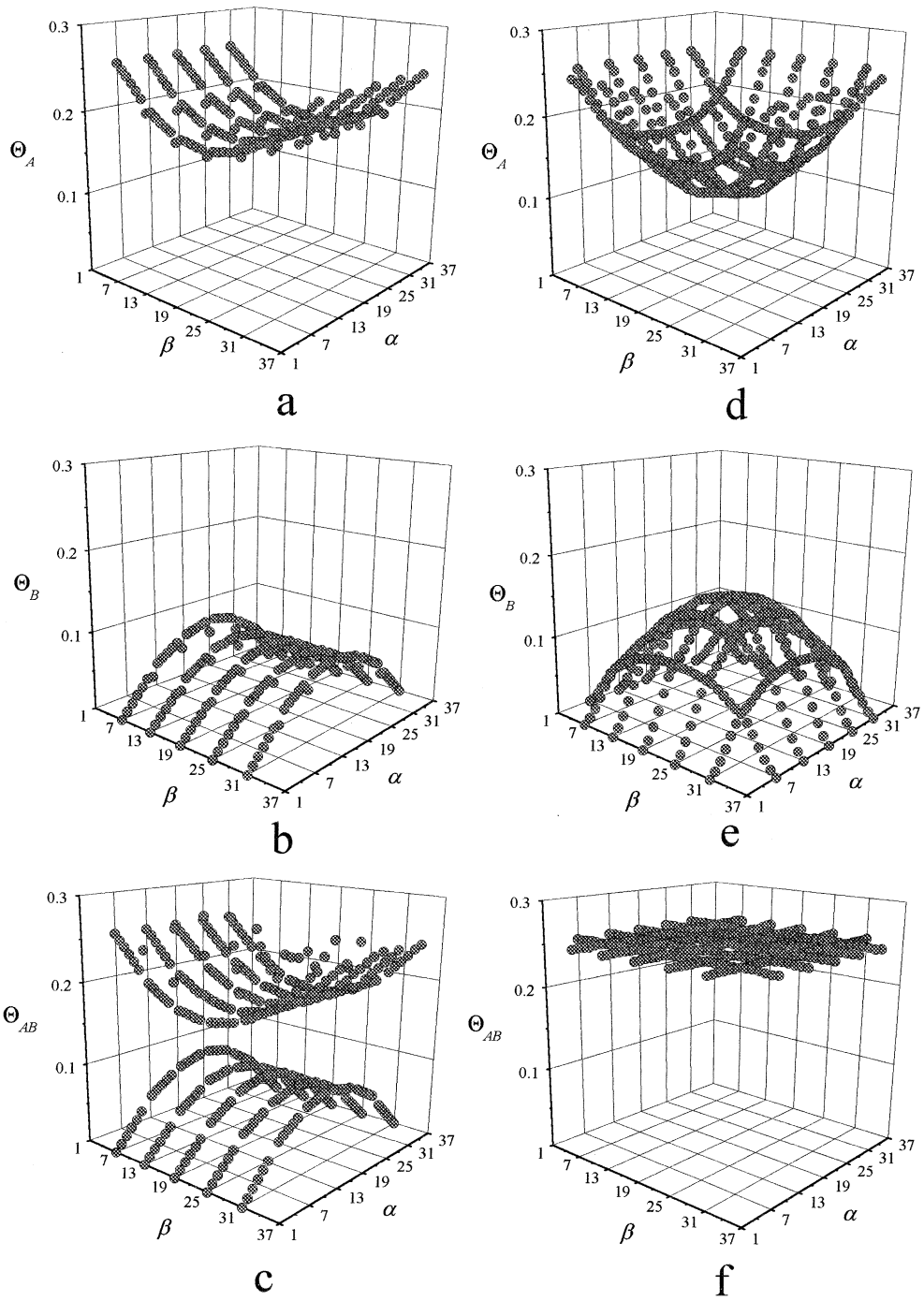

Figure 4. Concentration profiles of the A molecules (a and d), of the B molecules (b and e), and of both molecules (c and f) in the α and β channels for the reaction probability $\kappa_c = 0.01$ and for the initial lattice occupation $\langle\Theta_A(t = 0)\rangle = 0.25$ in the case of the MTC system (a−c) and the REF system (d−f).

probabilities. In the extreme case of reaction probability $\kappa_c = 1$ in the MTC system, A molecules can only be found in the first segments of the α channels, whereas B molecules are only found in the two outermost β channels, respectively. This is a simple consequence of the fact that the A molecules are converted into B molecules with absolute certainty in the very first channel intersections they get to after having entered the network. It is remarkable that for high reactivity the product molecules B in the MTC system attain much higher concentrations than the initially established equlibrium concentration of, in this case, $\langle\Theta_A(t = 0)\rangle = 0.25$. These high concentrations give rise to extremely large concentration gradients toward the end of the β channels. They are the consequence of the model-induced "valve effect" in the intersections: once being transferred from A to B species, the molecules cannot use the same way back to outside, which they just have used for propagating into the network interior.

Averaging the mean concentrations over all lattice sites or over all sites of a defined type of lattice points as the intersection points (subscript c)

$$\langle\Theta_i\rangle = \frac{1}{m_{tot}}\sum_{k=1}^{m_{tot}}\Theta_{i,k};\ \langle\Theta_{c,i}\rangle = \frac{1}{m_{c}}\sum_{s=1}^{m_{c}}\Theta_{i,s};\ i = A,B,AB \quad (8)$$

one can obtain the average site occupancies of the molecules *A*

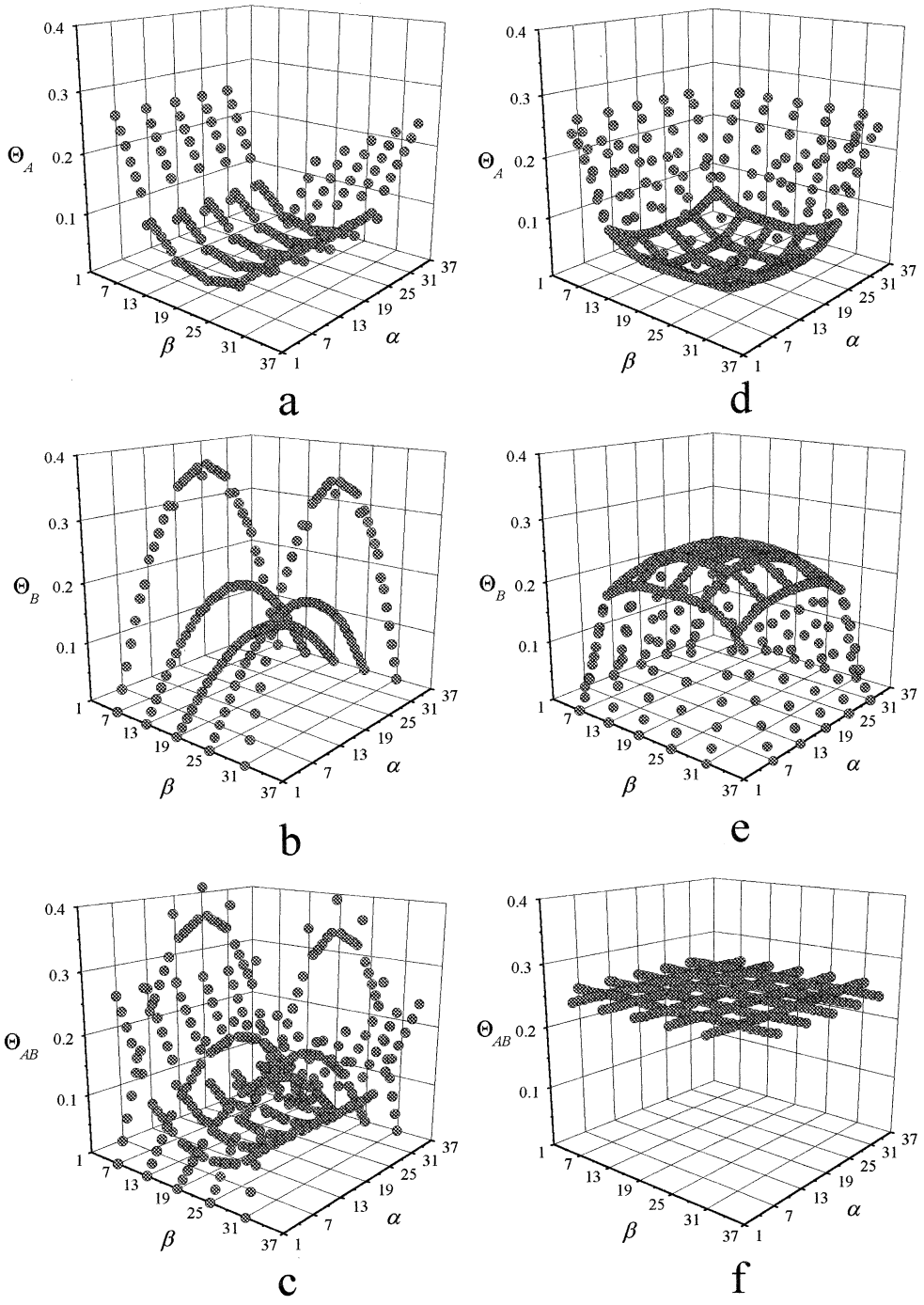

Figure 5. Same concentration profiles as in Figure 4 but for the reaction probability $\kappa_c = 0.1$.

and *B* and of their sum, which are denoted by $\langle\Theta_A\rangle$, $\langle\Theta_{A,c}\rangle$, $\langle\Theta_B\rangle$, $\langle\Theta_{B,c}\rangle$ and $\langle\Theta_{AB}\rangle$, $\langle\Theta_{AB,c}\rangle$. Figures 7−9 illustrate such average occupations as a function of the reaction probability κ_c. Figure 7 shows these quantities for a lattice of $n = 5$, $l = 5$ and for the initial occupation of the lattice $\langle\Theta_A(t = 0)\rangle = 0.25$ in the cases of the MTC (Figure a) and the REF system (Figure 7b). In the REF system (Figure 7b), the total concentration $\langle\Theta_{AB}^{REF}\rangle$ remains equal to 0.25, independent of the reactivity. This is the immediate consequence of the fact that the A and B molecules behave completely identical, so that any conversion of A to B cannot affect the overall behavior.[19]

In the MTC system, without any reaction, eq 6 would yield a concentration of A-type molecules equal to $\langle\Theta_A^{MTC}(\kappa_c = 0)\rangle = 0.1341$. This is also the total concentration $\langle\Theta_{AB}^{MTC}(\kappa_c = 0)\rangle$, because without reaction there were no B type molecules. For the smallest considered reaction rate $\kappa_c = 0.001$, not unexpectedly, the simulations yield the identical value $\langle\Theta_A^{MTC}(\kappa_c = 0.001)\rangle = 0.1341$. It is interesting to note that under the conditions chosen for the representation of Figure 7, similarly as in the REF system, also $\langle\Theta_{AB}^{MTC}\rangle$ remains essentially unaffected by further increasing reactivity. In contrast to the REF system, the total occupation of the intersections of the MTC system, $\langle\Theta_{AB}^{MTC}\rangle$, is notably higher than for the site average, $\langle\Theta_{AB}^{MTC}\rangle$. This is a consequence of the fact that in the MTC system the sites in the intersections may be occupied by both the A and B molecules, whereas the remaining sites may be occupied by either A or B molecules. Because this distinction

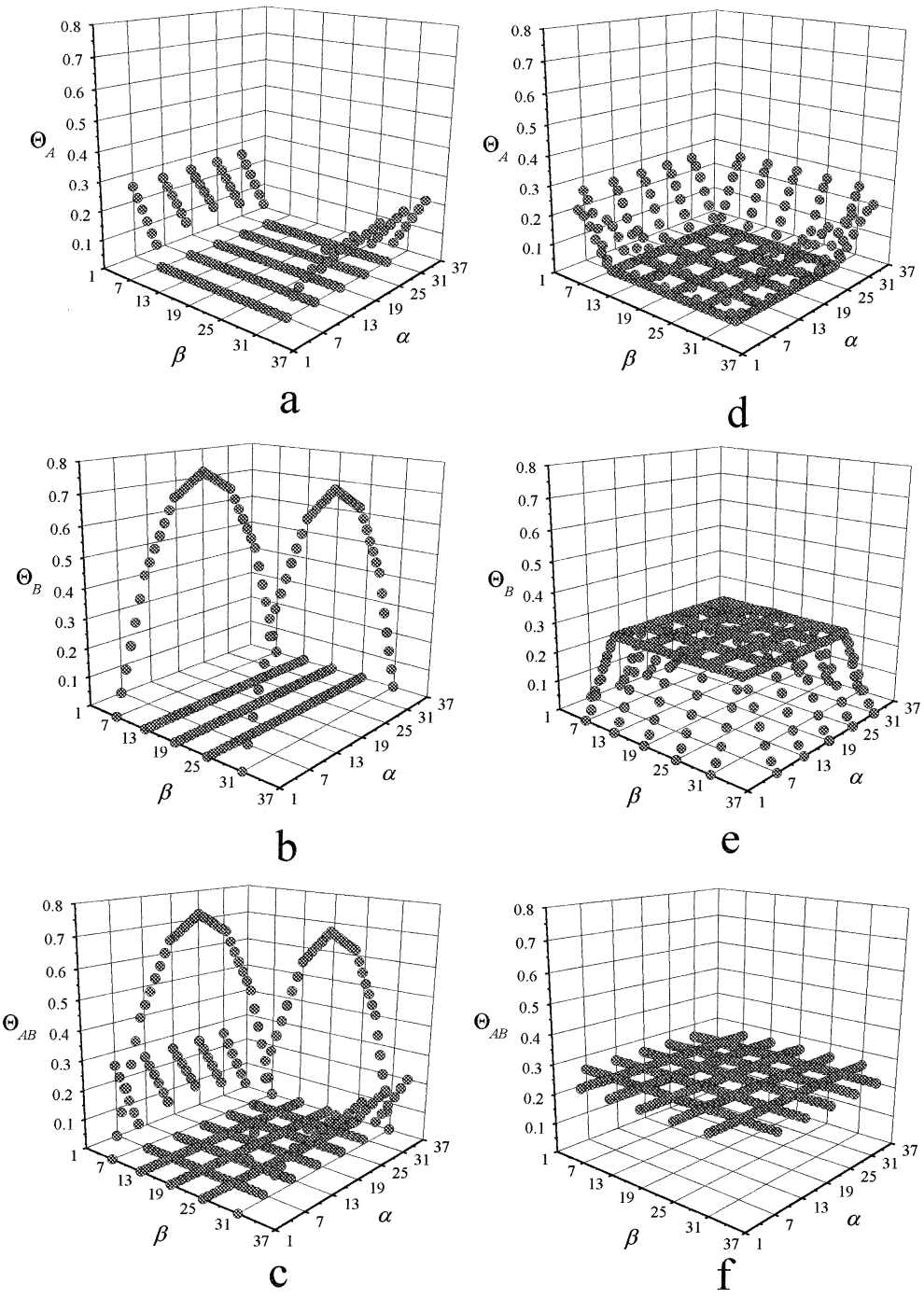

Figure 6. Same concentration profiles as in Figure 4 but for the reaction probability $\kappa_c = 1$.

does not exist in the REF system, there is no difference in the total occupation numbers of the sites in the intersections and the channel segments leading to $\langle\Theta_{AB}^{REF}\rangle \equiv \langle\Theta_{AB,c}^{REF}\rangle$. As to be expected, in both the REF and MTC systems, the concentration of B molecules increases with increasing reactivity κ_c, at the expense of the A molecules. Also not unexpectedly, this tendency is more pronounced for the concentrations in the intersections, i.e., on the active sites.

Figure 8 shows the mean occupancies $\langle\Theta_A\rangle$, $\langle\Theta_{A,c}\rangle$, $\langle\Theta_B\rangle$, $\langle\Theta_{B,c}\rangle$ and $\langle\Theta_{AB}\rangle$, $\langle\Theta_{AB,c}\rangle$ for the same lattice of the MTC system, but for the much larger initial occupation $\langle\Theta_A(t = 0)\rangle = 0.75$. In comparison with the representation in Figure 7a, the total concentration in the channel intersections as well as the mean total concentration over all lattice sites is now found to notably decrease with increasing reactivity. As a consequence of the large initial concentration ($\langle\Theta_A(t = 0)\rangle = 0.75$), the "valve effect" cannot lead to a dramatic enhancement in the site population of the outermost β channels (which is clearly limited to $\Theta = 1$) as exemplified for $\langle\Theta_A(t = 0)\rangle = 0.25$ in Figure 6b. Therefore, the depletion of concentration in the inner sites of the network (cf. Figures 5a−c and, in particular, 6a−c) are by far not compensated anymore by the concentration enhancement in the outermost β channels.

Figure 9 summarizes the representations of the total concentrations over the lattice as a function of the reaction probability κ_c for different starting concentrations (which correspond to different rates of insertion of novel A molecules into the marginal sites of the α channels, i.e., to different external pressures) as well as for an enhanced network in the case of the MTC system. Note that in the case of the REF system all

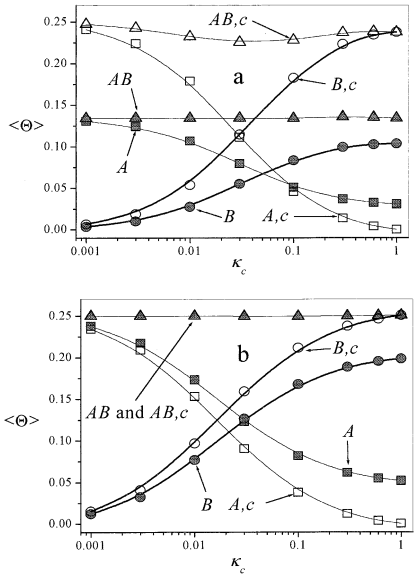

Figure 7. Average site occupancy of A molecules $\langle\Theta_A\rangle$, $\langle\Theta_{A,c}\rangle$ (filled and open squares) and B molecules $\langle\Theta_B\rangle$, $\langle\Theta_{B,c}\rangle$ (filled and open circles), as well as their sum $\langle\Theta_{AB}\rangle$, $\langle\Theta_{AB,c}\rangle$ (filled and open triangles) for the total lattice (filled symbols) and for only the intersection points (open symbols) for a lattice with $n = 5$, $l = 5$ and for an initial lattice occupation $\langle\Theta_A(t = 0)\rangle = 0.25$ in dependence on the reaction probability κ_c for the MTC system (a) and the REF system (b). For the REF system, there is $\langle\Theta_{AB}\rangle \equiv \langle\Theta_{AB,c}\rangle$. As a help for the eyes, the dependences for B molecules are represented by thicker lines.

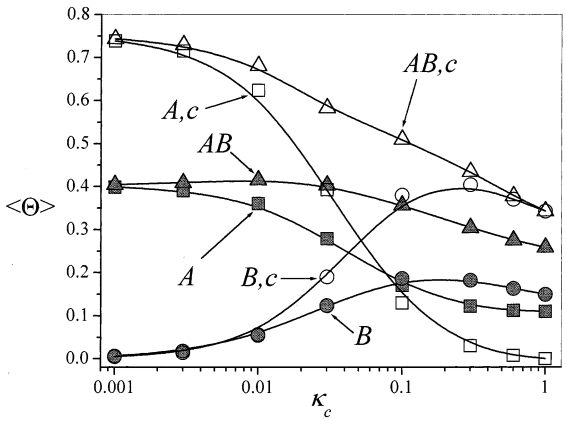

Figure 8. Average site occupancy of A molecules $\langle\Theta_A\rangle$, $\langle\Theta_{A,c}\rangle$ (filled and open squares) and B molecules $\langle\Theta_B\rangle$, $\langle\Theta_{B,c}\rangle$ (filled and open circles), as well as their sum $\langle\Theta_{AB}\rangle$, $\langle\Theta_{AB,c}\rangle$ (filled and open triangles) for the total lattice (filled symbols) and for only the intersection points (open symbols, upper index c) in dependence on the reaction probability κ_c for the MTC system. The lattice parameters are $n = 5$, $l = 5$, and $\langle\Theta_A(t = 0)\rangle = 0.75$.

representations would yield horizontal lines: Because all sites are equally accessible by both molecules A and B and because the microdynamic properties of both molecules are identical, the overall adsorption behavior does not depend on the percentage of A and B molecules and hence nor on their conversion rate. MTC systems therefore provide the intriguing feature of giving rise to isotherms of overall adsorption, which are a function of the intrinsic reactivity, irrespective of the fact that the involved molecules are microdynamically equivalent (one disregards their different affinity to α and β channels). Figure 9 reflects the previously discussed feature that the decrease in the overall loading with increasing reactivity is the larger, the larger is the initial occupation and the larger is the network (i.e., the smaller is the percentage of sites on the

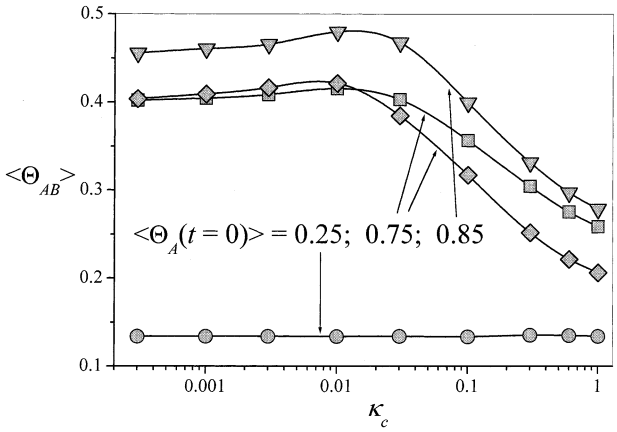

Figure 9. Average site occupancy of A and B molecules $\langle\Theta_{AB}\rangle$ for three lattices with $n = 5$, $l = 5$, and the different initial occupations $\langle\Theta_A(t = 0)\rangle = 0.25$ (circles), $\langle\Theta_A(t = 0)\rangle = 0.75$ (squares) and $\langle\Theta_A(t = 0)\rangle = 0.85$ (triangles) and for the lattice $n = 7$, $l = 5$ and the initial occupation $\langle\Theta_A(t = 0)\rangle = 0.75$ (diamonds) for the MTC system in dependence on the reaction probability κ_c.

outermost β channels). In addition, Figure 9 yields the remarkable feature that, before decreasing, overall mean concentrations may even pass a maximum. It is obviously a consequence of the sorption capacity of the β channels, which may contribute to the overall adsorption capacity as soon as a part of the A molecules are converted to B molecules.

V. Effectiveness of Catalytic Reactions and the Intracrystalline Mean Lifetime

According to the Thiele concept,[11,12,27] the so-called effectiveness factor

$$\eta = \langle\Theta_A\rangle/\langle\Theta_{AB}\rangle \tag{9}$$

of catalytic reactions, i.e., the percentage of molecules, which in a given instant of time may be subjected to a chemical reaction, may be represented as a function of a single quantity, which involves the intrinsic reactivity, the diffusivity, and a geometrical factor. This quantity is generally referred to as the Thiele modulus Φ and represented as[27]

$$\Phi = \frac{V}{S}\sqrt{\frac{\langle k\rangle}{D}} \tag{10}$$

with V and S denoting, respectively, the volume and the surface of the catalysts grain. $\langle k\rangle$ stands for its average reactivity, and D denotes the diffusion coefficient. For a slab of catalyst, it holds[27]

$$\eta = \frac{\tanh\Phi}{\Phi} \tag{11}$$

Quite generally, i.e., independent of the grain geometry, we have

$$\lim_{\Phi\to\infty}\eta = 1/\Phi \tag{12}$$

Intrinsic reaction and intercrystalline exchange are the two competing processes during conversion by catalytic particles. This fact becomes more obvious if the Thiele modulus is expressed in terms of the intracrystalline mean lifetime τ_{intra} rather than in terms of the diffusivity.[28] In the case of a slab catalyst of half-thickness a, e.g., one has $V/S = a$ and[11,27]

$$D = \frac{a^2}{3\tau_{\text{intra}}} \tag{13}$$

From eq 10 one finally obtains

$$\Phi = \sqrt{3\langle k\rangle \tau_{\text{intra}}} \tag{14}$$

Thus, it turns out that introducing the intracrystalline lifetime into eq 10 allows to simultaneously take account of the particle size and the intrinsic diffusivity.

In the case of the REF system, as an alternative to the analytical expression resulting from eq 13, i.e., independent of the geometry of the catalyst grain, the intracrystalline mean lifetime τ_{intra} can be calculated from the tracer exchange curve $\gamma(t)$. The function $\gamma(t)$ represents the relative amount of particles that have entered the system in the time interval 0... t or, equivalently, which have left the system in the same time interval. Thus, with the nomenclature introduced in section II, where at $t < 0$ only labeled, at $t \geq 0$, only unlabeled molecules have entered the system, we have

$$\gamma(t) = \frac{N_{\text{unlab}}(t)}{N_{\text{unlab}}(t) + N_{\text{lab}}(t)} = \frac{N_{\text{A,unlab}}(t) + N_{\text{B,unlab}}(t)}{N_{\text{A,tot}}(t) + N_{\text{B,tot}}(t)}$$

$$= 1 - \frac{N_{\text{A,lab}}(t) + N_{\text{B,lab,tot}}(t)}{N_{\text{A,tot}}(t) + N_{\text{B,tot}}(t)}; \quad 0 \leq \gamma(t) \leq 1 \tag{15}$$

Because in the REF system A and B molecules are supposed to behave identically, the tracer exchange curve as defined by eq 15 is completely independent of the intrinsic reactivity. In the case of no reactivity at all, eq 15 may therefore be replaced by the much simpler expression

$$\gamma(t) = \frac{N_{\text{A,unlab}}(t)}{N_{\text{A,tot}}} = 1 - \frac{N_{\text{A,lab}}(t)}{N_{\text{A,tot}}} \tag{16}$$

τ_{intra} is given by the relation[11,29]

$$\tau_{\text{intra}} = \int_0^\infty [1 - \gamma(t)]\, \mathrm{d}t = \frac{1}{N_{\text{A,tot}}(t=0)} \int_0^\infty N_{\text{A,lab}}(t)\, \mathrm{d}t \tag{17}$$

where the latter equation follows from eq 16.

In cases where the exchange time was too long, the simulations were stopped when the concentration of labeled molecules dropped to 5% of the initial value. The further development of the curve up to 1 was assumed to follow the function

$$\gamma(t > t_{\max}) = 1 - \exp(-t/\tau_{\text{extra}}) \tag{18}$$

with $\gamma(t_{\max}) = 0.95$ and the extrapolation parameter τ_{extra} determined by averaging over the last 50 values of $\gamma(t)$ before $\gamma = \gamma(t_{\max})$ via

$$\tau_{\text{extra}} = -\langle t/\ln[1 - \gamma(t)]\rangle \tag{19}$$

The intracrystalline mean lifetime determined from eq 17 by integrating up to only the value $\gamma(t_{\max})$ is denoted by $\tau_{\text{intra,1}}$. Continuing integration by making use of eq 18 leads to $\tau_{\text{intra,2}}$. As an example, Table 1 gives a comparison of the different values of $\tau_{\text{intra,1}}$ and $\tau_{\text{intra,2}}$, which result if $t_{\max}$ is deliberately chosen to yield $\gamma(t_{\max}) = 0.95$, 0.975, and 0.99, with the parameters $n = 7$, $l = 3$, $\langle k\rangle = 0.027273$, and $\langle \Theta_A(t=0)\rangle = 0.25$. It turns out that the extrapolation by means of eqs 18 and 19 only insignificantly influences the intracrystalline mean lifetime.

TABLE 1: Comparison of the Different Values of $\tau_{\text{intra,1and2}}$, Which Result if $t_{\max}$ Is Chosen to Yield $\gamma(t_{\max}) = 0.95$, 0.975, and 0.99, with the Exact Value (Corresponding to $\gamma(t_{\max}) = 1$) for the Lattice Parameters $n = 7$, $l = 3$, $\langle k\rangle = 0.027273$, and $\langle \Theta_A(t=0)\rangle = 0.25$, and Their Influence on the Thiele Modulus (eq 10)

$N_{\text{unlab,tot}}(t)/N_{\text{tot}}$	$\gamma(t_{\max})$	$\tau_{\text{intra,1}}$	$\tau_{\text{intra,2}}$	$\Phi(\tau_{\text{intra,2}})$
1	1	504.0406	504.0406	6.42181
0.99	0.9899684	494.9496	501.4210	6.40510
0.975	0.974952	480.2587	495.8229	6.36925
0.95	0.9500236	464.6754	495.0793	6.36447

Catalysts containing the channel network under study have to be considered as infinitely largely extended prisms with quadratic cross section rather than slab-like. In this case, an analytic expression of τ_{intra} may be deduced from the relation[29]

$$\tau_{\text{intra}} = \frac{4}{D\pi^2}\left(\frac{8}{\pi^2}\right)^3 \sum_{i=0}^{\infty}\sum_{j=0}^{\infty}\sum_{k=0}^{\infty} A(i,j,k,a,b,c) \tag{20}$$

with

$$A(i,j,k,a,b,c) = \frac{1}{(2i+1)^2(2j+1)^2(2k+1)^2\left[\left(\frac{2i+1}{a}\right)^2 + \left(\frac{2j+1}{b}\right)^2 + \left(\frac{2k+1}{c}\right)^2\right]} \tag{21}$$

for the intracrystalline lifetime in a rectangular parallelepiped of dimensions $2a$, $2b$, $2c$. With $a = b$ and $c \rightarrow \infty$, eq 21 simplifies to

$$A(i,j,k,a) = \frac{a^2}{(2i+1)^2(2j+1)^2(2k+1)^2[(2i+1)^2 + (2j+1)^2]} \tag{22}$$

Numerical evaluation of eq 20 with eq 22 and taking $L = 2a$ yields

$$\tau_{\text{intra}} = \frac{L^2}{28.454D} \tag{23}$$

Finally, with eq 10 and $V/S = L/4$ the Thiele modulus is found to be related to the mean intrinsic reactivity $\langle k\rangle$ and the intracrystalline lifetime τ_{intra} by

$$\Phi = \sqrt{1.7784\langle k\rangle \tau_{\text{intra}}} \tag{24}$$

We are going to use eqs 23 and 24 for a series of consistency checks of our results for the REF system.

(i) The diffusivity D of eq 23 must be expected to be given by the basic equation of random walk on square lattices[11]

$$D = \frac{l_{\text{cc}}^2}{4\tau_{\text{cc}}} \tag{25}$$

with l_{cc} and τ_{cc} denoting the distance between adjacent channel intersections and the meantime it takes a molecule to get from one channel intersection to an adjacent one. Figure 10 shows the values of τ_{cc} resulting from the MC simulations, as a function of the distance between adjacent intersections for the REF system. In our model, we have $l_{\text{cc}} = (l+1)\lambda$ (cf. Figure 1), where λ is the distance between two adjacent lattice sites. The straight lines in the double-logarithmic representations indicate

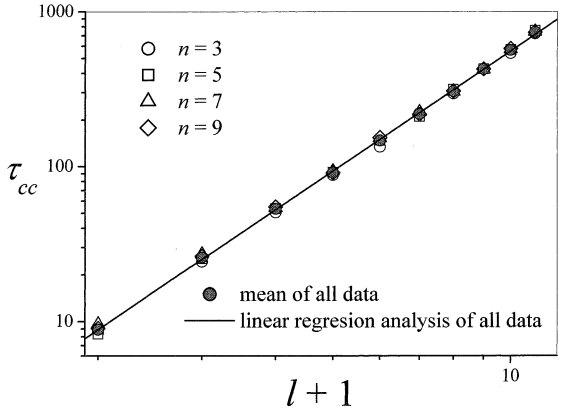

Figure 10. Mean time τ_{cc} of a molecule between two neighboring intersection points in the REF system with $n = 3$ (open circles), 5 (open squares), 7 (open triangles), and 9 (open diamonds) channels in either direction, as well as the mean (filled circles) taken over all values of n, calculated with $\langle k \rangle = 0$ and an initial lattice occupation $\langle \Theta_A(t = 0) \rangle = 0.25$, as function of the file length $l + 1$ between the intersection points. The straight line is the linear regression curve for all data. The values of τ_{cc} are represented in units of the time steps of simulation, i.e., the meantime between subsequent molecular jump attempts.

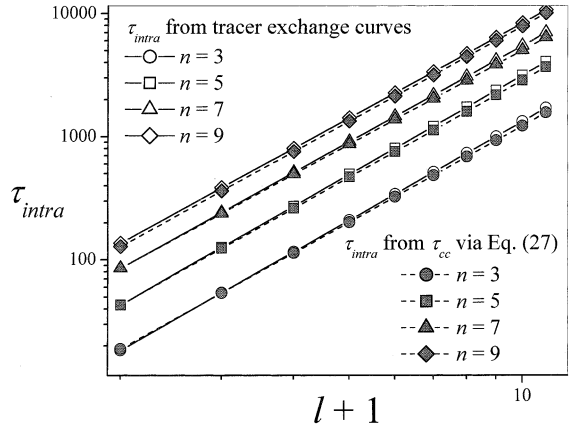

Figure 11. Mean intracrystalline residence time τ_{intra} (in units of the time step of simulation) of the molecules of type A in the REF system with $n = 3$ (circles), 5 (squares), 7 (triangles), and 9 (diamonds) and a total occupation of 0.25 as function of the file length $l_{cc}/\lambda = l + 1$ between two intersections, calculated from the tracer exchange curves (open symbols) and from the mean passage times between adjacent channel intersection by use of the modified Barrer formula, eq 27 (filled symbols).

a mutual relationship of the type

$$\tau_{cc} \propto (l + 1)^x = l_{cc}^x \tag{26}$$

Linear regression analysis yields an exponent $x = 2.57 \pm 0.02$ with a regression coefficient $r_{xy} = 0.99974$ independent of the number of considered channels. In contrast to the case of ordinary diffusion, where the mean traveling time along the channel segments from intersection to intersection scale with the square of their distance, the influence of this distance is now found to be more significant. This is in complete agreement with the situation known from single-file systems, where, for example, the mean lifetime in a channel scales with its third power, rather than with its second power as were the case for ordinary diffusion. In fact, molecular propagation from intersection to intersection in the REF system has to proceed under single-file conditions, because the molecules have to keep their order and there are no macroscopic concentration gradients. Thus, in any case, the scaling exponent correlating the exchange time τ_{cc} between the intersection sites and their distance $l + 1$ has to be expected to be notably larger than 2. On the other hand, one clearly cannot expect that it necessarily assumes the value of 3, because the mean lifetime of the molecules in a single, finite single-file system with fast exchange with the surrounding atmosphere on the marginal sites describes a different physical situation than molecular passage from intersection to intersection in a network of single-file systems, even if their distance (i.e., the intercept of relevance) coincides with the length of the finite single-files system. Thus, though the origin of the particular value of $x = 2.57$ for the scaling exponent is still unclear and has to remain the subject of further research, it is in qualitative agreement with the expected behavior.

(ii) Via eqs 25 and 23, the mean passage times τ_{cc} of Figure 10 may be transferred into the intracrystalline mean lifetimes by the relation

$$\tau_{intra} = \frac{(n + 1)^2}{7.1135} \tau_{cc} \tag{27}$$

Figure 11 compares the intracrystalline mean lifetimes resulting from eq 27 with the values following from an analysis of the tracer exchange curves via eq 17. The satisfactory agreement between the two sets of data confirms that the intracrystalline mean lifetime in the REF system may in fact be discussed in terms of the mean passage time between adjacent intersections.

Under diffusion control (i.e., for sufficiently large values of the Thiele modulus Φ), with eqs 12 and 14, the effectiveness factor of the catalytic reaction turns out to decrease with increasing intracrystalline mean lifetimes. In the case of the REF system (see Figures 10 and 11), the intracrystalline mean lifetime is found to increase with the power of 2.57 rather than only with the square of the distance between the intersections as it would be the case for normal diffusion. The anomalous power of 2.57 has been shown to be caused by the (coinciding) scaling exponent of molecular passage from intersection to intersection, which has been attributed to the single-file conditions under which molecular propagation occurs in the REF system.

It has been visualized by Figures 4−6, parts c and f in each, that, as a most significant feature, the overall concentration in REF systems is spatially constant, whereas the MTC system operates under the condition of permanent concentration gradients along both channel types, viz. along the α channels into the catalyst and along the β channels out of the catalyst. Therefore, molecular transport in the MTC system may proceed according to the laws of transport diffusion, where the single-file confinement is of no relevance.[28,30] Uptake of the reactant molecules into the catalyst and release of the product molecules into the surrounding atmosphere, therefore, occur under the conditions of ordinary diffusion with a (transport) diffusivity coinciding with the single-particle self-diffusivity.[11] Thus, the exchange times tend to scale with the second power of l rather than with 2.57, as observed with the REF systems. In complete agreement with these different dependencies, with increasing intersection separations, the effectiveness factors as compared in Figure 3a are found to decrease more rapidly in the REF system, leading to a relative gain of the MTC system.

VI. Release of the "Hard" MTC Conditions

One should have in mind that the present simulations have been carried out for rationalizing the possibility of reactivity enhancement by MTC. The peculiarities of molecular transport under single-file conditions have in fact been recognized as a possible mechanism for reactivity enhancement by MTC. By

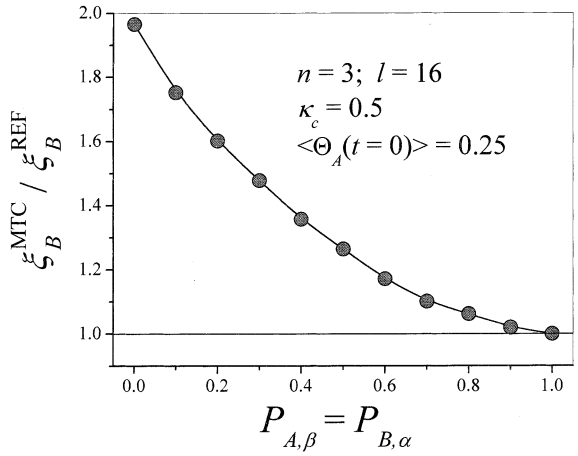

Figure 12. Benefit ξ_B^{MTC}/ξ_B^{REF} of the MTC system in comparison with the REF system for $n = 3$, $l = 16$, $\kappa_c = 0.5$, and $\langle\Theta_A(t = 0)\rangle = 0.25$ in dependence on the probabilities $P_{A,\beta}$ that an A molecule enters a β channel and the probability $P_{B,\alpha}$ that a B molecule enters an α channel (which, for the sake of simplicity, are assumed to be identical). The limiting cases $P_{A,\beta} = P_{B,\alpha} = 0$ and 1 represent the "hard" MTC system so far considered in this study and the REF system, respectively.

doing so, we have deliberately chosen the most simple conditions, i.e., a network of only two arrays of parallel channels, and the "hard" MTC condition, i.e., the total exclusion of the accommodation of A molecules in the β channels and, vice versa, of B molecules in the β channels. It is demonstrated by Figure 12 that partially abandoning the "hard" MTC condition may afford effective reactivities, which are still notably superior to the values of the REF system.

VII. Discussion

The reasoning of the previous section is based on the assumption that the Thiele concept may serve as a suitable guideline for the effectiveness of catalytic reactions in the MTC and REF systems. The Thiele concept has been derived for a continuum with uniform propagation and conversion probabilities.[11,12] In the presently considered systems, this is not the case anymore. The less severe deviations have to be anticipated for the REF system, in which site uniformity is violated by the fact that molecular jumps and conversion may simultaneously occur only in the intersections, whereas there is no conversion on the sites on the connecting segments. In addition, in the MTC system uniformity of particle propagation is violated by a second item: reactant and product molecules are obliged to propagate along different pathways.

In view of this consideration, application of the Thiele concept might be expected to yield agreement with the DMCS data in a qualitative way only. Figure 13, parts a and b, provides such a comparison by following two different routes. Figure 13a represents the effectiveness factor (η) in the conventional way by expressing the mean value of ratio between the occupation by A-type molecules and all molecules, taken over all sites (eq 9). Taking into account that in reality the effectiveness of conversion only depends on the occupation of the sites in the intersections, the modified effectiveness factor (η_c) plotted in Figure 13b represents the respective population ratios only on these sites. In complete analogy to eq 9, the modified effectiveness factor is defined by the relation

$$\eta_c = \langle\Theta_{A,c}\rangle/\langle\Theta_{AB,c}\rangle \qquad (28)$$

The modified effectiveness factor necessitates the introduction

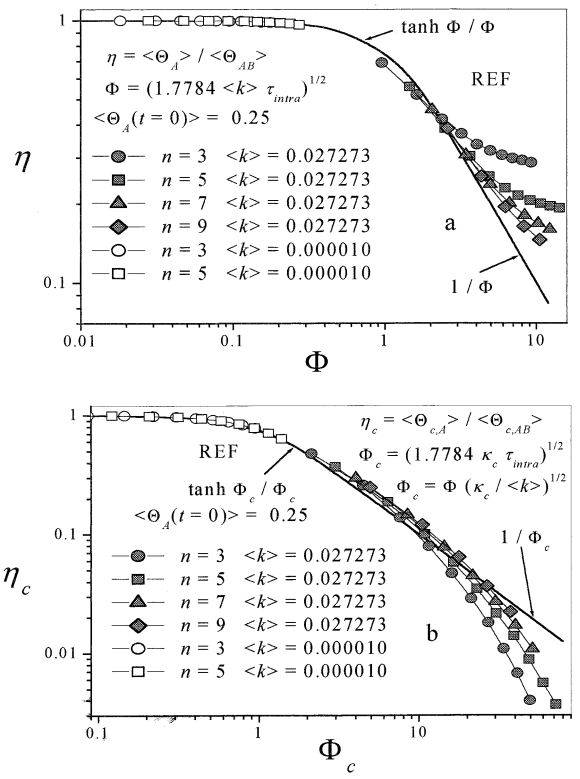

Figure 13. Effectiveness factor η (cf. eq 9, Figure 13a) and modified effectiveness factor η_c (cf. eq 28, Figure 13b) as function of the Thiele modulus Φ (cf. eq 24) and modified Thiele modulus Φ_c (cf. eq 29) respectively, for different lattices of the REF system with $n = 3$ ($l = 1, 2, ..., 10$; circles), $n = 5$ ($l = 1, 2, ..., 10$; squares), $n = 7$ ($l = 1,2, ..., 7$; triangles), and $n = 9$ ($l = 1, 2, ..., 5$; diamonds) α and β channels. All data are valid for an initial lattice occupation $\langle\Theta_A(t = 0)\rangle = 0.25$ and for the two average reactivities $\langle k\rangle = 0.027273$ (filled symbols) and $\langle k\rangle = 0.00001$ (open symbols) of the lattices. The data were compared with the corresponding analytical dependence for a slab catalyst (eq 11).

of a modified Thiele modulus Φ_c, which by use of the relation

$$\Phi_c = \sqrt{1.7784\kappa_c\tau_{intra}} = \Phi\sqrt{\kappa_c/\langle k\rangle} \qquad (29)$$

instead of eq 24 is based on the reactivity on the considered sites, i.e., on κ_c, rather than on their mean value $\langle k\rangle$ over all sites.

As indicated in the inserts to the figures, the respective effectiveness factors η and η_c have been determined for a multitude of parameter sets with the number l of sites between adjacent intersections varying between 1 and 10 for essentially any considered data pairs n and $\langle k\rangle$. It turns out that, at least in a qualitative way, the data tend to follow the dependence predicted by the Thiele concept with, for example, eq 11 as an analytical expression between the two limiting cases $\eta(\Phi = 0)$ and $\eta(\Phi \gg 1) = 1/\Phi$, which hold quite generally, irrespective of the considered geometry.[11,24] The systematic deviations from the Thiele dependence $\eta = 1/\Phi_{(c)}$ as appearing from the representation in Figure 13 with $\Phi_{(c)}$ values notably exceeding $\Phi_{(c)} = 1$ are not unexpected in view of the above-discussed inherent differences. Interestingly enough, depending on the chosen representation, $\eta(\Phi)$ or $\eta_c(\Phi_c)$, the deviations tend to higher or lower values, respectively. As a particularly important feature, in both cases, the approximation by the Thiele concept becomes increasingly better with the increasing number of channels. This finding is in complete agreement with the expected behavior because with increasing channel numbers the

considered channel network will doubtless be increasingly better described by a continuum model as provided by the Thiele concept.

Though an analogous treatment of the MTC system has to remain a subject of further research, it seems justified, therefore, to apply the Thiele concept at least in a qualitative way for rationalizing the observed differences in the effectiveness of the REF and MTC systems.

Because according to eq 9 the effectiveness factor refers to the total concentration $\langle\Theta_{AB}\rangle$ on the reactive sites, the catalytic efficiency of the REF and MTC networks as compared in parts a and b of Figure 3 is clearly a function of both the effectiveness factor and the actual concentration of the reactive sites. The comparison of these concentrations in parts a and b of Figure 7 does in fact reveal that under the considered conditions ($n = l = 5$, $\langle\Theta_A(t=0)\rangle = 0.25$) in both cases the total concentration of the active sites (i.e., $\langle\Theta_{AB,c}\rangle$) is close to 0.25. Under these conditions, a comparison of the effective reactivity of the REF and MTC systems may clearly exclusively be based on the respective effectiveness factors. Figures 5, 6, 8, and 9 show, however, that with further increasing reactivity and/or loading, $\langle\Theta_{AB,c}\rangle$ of the MTC system becomes notably smaller than in the REF system. This is an immediate consequence of the inherent confinement of the MTC system, which tends to keep the concentration of the central part much lower than in the marginal sites. This effect clearly increases with increasing channel numbers, leading to the dramatic decrease in the effective reactivity in the MTC system, in comparison with the REF system, as shown in Figure 3b.

VIII. Outlook and Conclusion

As a consequence of the artificial maintenance of coinciding overall concentrations in both systems, in previous studies[18−20] the advantage of the MTC system over the REF system has been overestimated. The present study clarifies under which conditions the superiority of the MTC system versus the REF system is maintained even if the artificial requirement of coinciding mean sorbate concentrations is abandoned. It turns out that the MTC system becomes progressively beneficial over the REF system with increasing file lengths between the intersection points. Thus, the benefit of the MTC system is found to be purchased by (i) stronger transport inhibition and (ii) a reduced density of active sites (because in the model considered the sites in the channel segments, being accessible by only one type of molecules, had to be required to be inactive for molecular conversion). Because of these two items, at a first glance, the findings of this study appear not to be in favor of the MTC principle, from a practical point of view. With Figure 12, it has been demonstrated, however, that even by partially abandoning the "hard" MTC condition effective reactivities may be attained, which are still notably higher than those in the REF system.

Because all practically feasible systems (cf., for example refs 8−10) are expected to possess features of "soft" MTC, the findings represented in Figure 12 are of particular relevance for the practical exploitation of MTC. Moreover, in the soft MTC systems, catalytic conversions are clearly allowed to occur in all sites and not exclusively on the channel intersections. Thus, again as a result of substantial practical impact, the density of the catalytically active sites may be substantially enhanced in comparison with the so far considered "hard" MTC systems.

Finally, the three-dimensional space offered by nature may be readily assumed to be able to host more complex channel networks, which may additionally favor the effective reactivity under MTC conditions. There is in fact ample space for further research in search of the optimum conditions for reactivity enhancement by molecular traffic control in single-file networks, where besides reactivity enhancement the prospects of also selectivity improvement is most likely to turn out to be a profitable issue.

Acknowledgment. Financial support by the Deutsche Forschungsgemeinschaft and Fonds der Chemischen Industrie is gratefully acknowledged. We are obliged to Armin Bunde, Giessen, and Gunter Schütz, Jülich, for numerous stimulating discussions and to the two reviewers for valuable comments and suggestions.

References and Notes

(1) Riekert, L. In *Advances in Catalysis*; Eley, D. D., Pines, H., Weisz, P. B., Eds.; Academic Press: New York, 1970; Vol. 21, p 281.
(2) Kukla, V.; Kornatowski, J.; Demuth, D.; Girnus, I.; Pfeifer, H.; Rees, L. V. C.; Schunk, S.; Unger, K. K.; Kärger, J. *Science* **1996**, *272*, 702.
(3) Kärger, J., Heitjans, R., Haberlandt, R., Eds.; *Diffusion in Condensed Matter*: Vieweg: Braunschweig, Wiesbaden, 1998.
(4) Wei, Q.-H.; Bechinger, C.; Leiderer, P. *Science* **2000**, *287*, 625.
(5) Derouane, E. G.; Gabelica, Z. *J. Catal.* **1980**, *65*, 486.
(6) Derouane, E. G. *Appl. Catal., A* **1994**, *115*, N2.
(7) Baerlocher, Ch.; Meier, W. M.; Olson, D. H. *Atlas of Zeolite Structure Types*; Elsevier: London, 2001.
(8) Snurr, R. Q.; Kärger, J. *J. Phys. Chem. B* **1997**, *101*, 6469.
(9) Clark, L. A.; Ye, G. T.; Snurr, R. Q. *Phys. Rev. Lett.* **2000**, *84*, 2893.
(10) Clark, L. A.; Ye, G. T.; Gupta, A.; Hall, L. L.; Snurr, R. Q. *J. Chem. Phys.* **1999**, *111*, 1209.
(11) Kärger, J.; Ruthven, D. V. *Diffusion in Zeolites and Other Microporous Solids*; Wiley: New York, 1992.
(12) Chen, N. Y.; Degnan, T. F.; Smith, C. M. *Molecular Transport and Reaction in Zeolites*; VCH: New York, 1994.
(13) Pope, C. G. *J. Catal.* **1981**, *72*, 174.
(14) Derouane, E. G. *J. Catal.* **1981**, *72*, 177.
(15) Keil, F. *Diffusion und chemische Reaktion in der Gas/Feststoff-Katalyse*; Springer: Berlin, 1999; p 200.
(16) Weitkamp, J.; Ernst, S.; Puppe, L. In *Catalysis and Zeolites*; Weitkamp, J., Puppe, L., Eds.; Springer: Berlin, 1999; p 346.
(17) Rödenbeck, C.; Kärger, J.; Hahn, K. *J. Catal.* **1995**, *157*, 656.
(18) Neugebauer, N.; Bräuer, P.; Kärger, J. *J. Catal.* **2000**, *194*, 1.
(19) Bräuer, P.; Kärger, J.; Neugebauer, N. *Europhys. Lett.* **2001**, *53*, 8.
(20) Kärger, J.; Bräuer, P.; Pfeifer, H. *Z. Phys. Chem.* **2000**, *214*, 1707.
(21) Rödenbeck, C.; Kärger, J. *J. Chem. Phys.* **1999**, *110*, 3970.
(22) Keil, F. J.; Krisna, R., Coppens, M.-O. *Rev. Chem. Eng.* **2000**, *16*, 71.
(23) Nelson, P. H.; Kaiser, A. B.; Bibby, D. M. *J. Catal.* **1991**, *127*, 101.
(24) Nelson, P. H.; Bibby, D. M.; Kaiser, A. B., *Zeolites* **1991**, *11*, 337.
(25) Marsaglia, G.; Zaman, A. *Statist. Prob. Lett.* **1990**, 9.1, 35.
(26) Rödenbeck, C. Ph.D. Thesis, Faculty of Physics and Earth Science, University of Leipzig, Leipzig, Germany, 1995.
(27) Aris, R. *The Mathematical Theory of Diffusion and Reaction in Permeable Catalysts*; Clarendon Press: Oxford, 1975.
(28) Kärger, J.; Petzold, M.; Pfeifer, H.; Ernst, S.; Weitkamp, J. *J. Catal.* **1992**, *136*, 283.
(29) Barrer, R. M. *Zeolites and Clay Minerals as Sorbents and Molecular Sieves*; Academic Press: London, 1978; p 272.
(30) Kutner, R. *Phys. Lett.* **1981**, *81A*, 239.